JOURNAL OF SOLID STATE CHEMISTRY **138,** 334–341 (1998)
ARTICLE NO. SC987793

Ordering of Metal Atoms in Wurtzite and Sphalerite Structures

J. Hauck and K. Mika

Institut für Festkörperforschung, Forschungszentrum Jülich, D 52425 Jülich, Germany
E-mail: k.mika@fz-juelich.de

Received December 8, 1997; in revised form February 2, 1998; accepted February 17, 1998

The Zn atoms of the wurtzite or sphalerite structure (ZnS) exhibit a hexagonal or cubic close packing with $T_1 = 12$ nearest and $T_2 = 6$ next-nearest neighbors. Ordered compounds such as $CuFeS_2$, $SbCu_3S_4$, and $SnFeCu_2S_4$ can be characterized by the self-coordination numbers T_1, T_2, and T_3 of the metal atoms and plotted on structural maps with coordinates T_1, T_2, T_3. The three compounds, for example, are at the right border of the map which satisfies Pauling's electrovalence rule. The interaction between metal atoms is repulsive. Other compounds such as $GeCu_2Se_3$, β-Ga_2Se_3, and α-LiSiNO are at different positions of the structure map with attractive interactions between metal atoms and violate Pauling's rule. Some new crystal structures and appropriate metal atoms are selected for the synthesis of new compounds. © 1998 Academic Press

1. INTRODUCTION

ZnS can crystallize in the hexagonal wurtzite or the cubic sphalerite structure. The Zn atoms of the wurtzite structure form a hexagonal close packing with the sequence of layers *AB* (Fig. 1). The metal atoms of sphalerite are cubic close packed with the sequence *ABC*. Many other stacking variants such as ZnS 4H or ZnS 9R, with the sequences *ABAC* or *ABABCBCAC*, can occur depending on temperature and composition (1, 2). The ordering of metal atoms corresponds to the Mg (*AB*), Cu (*ABC*), α-Nd (*ABAC*), or α-Sm (*ABABCBCAC*) crystal structure (2, 3). The sulfur atoms of ZnS are on tetrahedral sites in such a way that they are coordinated by four Zn atoms and that each Zn atom is coordinated by four S atoms. The Zn and S positions of sphalerite and wurtzite correspond to the carbon positions of diamond and the rare hexagonal diamond (lonsdaleite). Therefore the family of structures is called adamantane structures. The Zn and S atom positions of the adamantane structures can be occupied by different atoms in ternary or quaternary compounds (Table 1). Al_2CO and $\square Si_2N_2O$ are among the few examples of S substitution that exhibit a random distribution of C and O or N and O; in most cases, vacancies □ or metal atoms at Zn positions are ordered (1, 2).

In the present investigation the crystal structures will be characterized by the self-coordination numbers of the individual metal atoms. In that case the ordered adamantane structures can be compared with ordered hexagonal- or cubic-close-packed structures and can be analyzed for attractive or repulsive interactions between nearest and next-nearest metal atoms by the Ising model (3, 4). The correlation between structure and interactions between metal atoms will be demonstrated for the square-planar lattice (Fig. 2). The structural maps of hcp and ccp alloys (Fig. 3) which were determined before (3) show the location of the different adamantane structures. The occurrence of homometric and homologous structures at identical positions of the structure map and the combination of structural units at the boundary lines of the map will be explained.

2. SQUARE-PLANAR LATTICE

The numerical procedure for obtaining a structure map with a correlation between the different structures will be outlined for a single tetragonal layer occupied by *M* and *N* atoms in the ratio M_xN_y with $y/x \geq 1$ (Fig. 2). The procedure contains the following steps:

(1) A large variety of structures is obtained by a systematic variation of the unit cell (3).

(2) A maximum of 50% of the metal positions are occupied with *M* atoms. The structures at higher *M* content are identical by exchange of the *M* and *N* atoms.

(3) The different crystal structures can be characterized by the self-coordination numbers (self-CN) T_1, T_2, and T_3 of the *M* atoms with other *M* atoms in the first, second, and third coordination shells and the ratio y/x of *N* and *M* atoms, e.g., the notation 2 0 4;1 is used for the structure with $T_1 = 2$ metal atoms *M* at distance *a*, no *M* atoms in the second coordination shell, $T_3 = 4$ *M* atoms at distance 2*a*, and $y/x = 1$. $T_1^{max} = T_2^{max} = T_3^{max} = 4$ are the maximum self-CN of the tetragonal layer. The self-CN of each cell are averaged for structures which have differently coordinated *M* atoms; e.g. the 0 4 2, 2 0 2, and 1 2 4 (twice) self-CN of the four *M* atoms are averaged in the 1 2 3;1 structure.

0022-4596/98 $25.00

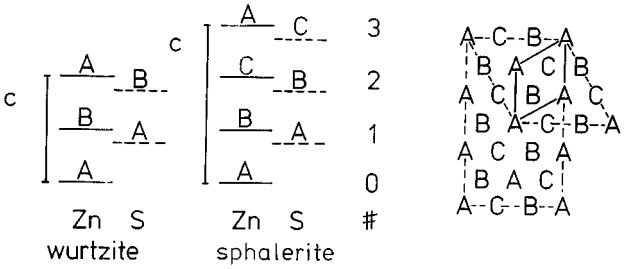

FIG. 1. Close-packed hexagonal layers of spheres on A positions (right). The next hexagonal layer can be placed either on B or C positions. Sequence of Zn and S layers in wurtzite and sphalerite structure and Zn layer number (left).

(4) The crystal structures characterized by the self-CN T_1, T_2, and T_3 and a fixed composition y/x can be plotted as single points in a T_1,T_2,T_3 coordinate system or as projection in the T_1,T_2 plane as outlined for $T_1T_2T_3;1$ structures in Fig. 2. All structures are found to fall within a triangle, with the three structures 4 4 4;(1), 2 0 4;1, and 0 4 4;1 at the corners. The structure 4 4 4;(1) with the composition given by (1) in parentheses can only be obtained in the limit of very large unit cells, because the boundary line between the M and N clusters prevents an exact realization 4 4 4;1 for finite cells.

(5) The structures with $y/x = 1$ shown on the structure map can be considered as a combination of the variously shaded squares containing different numbers of M atoms and different configurations (*cis* and *trans*) at the occupation of two positions (Fig. 2). The 0 4 4;1 and 2 0 4;1 structures at the right and upper corners of the triangle (Fig. 2) consist of squares containing two M atoms in *trans* or *cis* configuration, respectively. The other structures at the right side with the same composition as, for example, 1 2 3;1 can be obtained by combination of the two structural units with different shadings. The 4 4 4;(1) structure at the left corner of the triangle can be considered as complete segregation of M and N atoms with complete occupancy of the squares by M or N atoms, respectively. These structural units can be

TABLE 1

Self-Coordination Numbers and Concentrations $T_1T_2T_3;r$ ($r=(n-z)/z$) of Metal Atoms (or Vacancies □) in $A_uB_vC_wD_yX_n$ ($z=u, v, w$ or y and $n=u+v+w+y$) in Sphalerite- and Wurtzite-Related Structures (S and W)

Compound	$T_i(A)$	$T_i(B)$	$T_i(C)$	$T_i(D)$	Alloy
	A. Sphalerite-related structures				
ZnS, $(□Ga_2)Te_3$	12 6 24;(1)				Cu
$(AgGa)Se_2$, $(AsCu_3)Se_4$					
$(□Cu_{0.4}In_{1.2})Se_2$					
$(□FeGa_2)Se_4$					
S-AB_3X_4	0 6 0;3				$AuCu_3$
S-AB_3X_4	0 5 4;3				$ZrAl_3$
$SbCu_3S_4$	0 4 8;3				$TiAl_3$
S-ABX_2	4 6 8;1				CuAu
S-ABX_2	4 5 12;1a				
S-ABX_2	4 5 12;1b				
$CuFeS_2$	4 4 16;1				U Pb
$□CdIn_2Se_4$	0 6 0;3	0 6 0;3	4 6 8;1		$PdAuCu_2$
$SnFeCu_2S_4$	0 4 8;3	0 4 8;3	4 6 8;1		
β-$□HgCu_2I_4$	0 4 8;3	0 4 8;3	4 6 8;1		
□(Mn, In)(Mn, In)$_2$Te$_4$	0 4 8;3	0 4 8;3	4 6 8;1		
$□CdGa_2S_4$	0 4 8;3	0 4 8;3	4 4 16;1		
$SnZnCu_2S_4$	0 4 8;3	0 4 8;3	4 4 16;1		
$□_2AgIn_5Se_8$	0 4 8;3	0 4 0;7	6.4 5.6 12.8;0.6		
S-ABC_2X_4	0 6 0;3	0 4 8;3	4 5 12;1a		
S-$ABCDX_4$	0 6 0;3	0 4 8;3	0 6 0;3	0 4 8;3	
S-ABX_2	9 3 12;1				
S-ABX_2	5 3 12;1				
S-ABX_2	6 2 12;1a				
S-ABX_2	6 2 12;1b				
In(Ga, Al)P_2	6 0 12;1a				CuPt,a
S-ABX_2	6 0 12;1b				CuPt,b
$GeCu_2Se_3$	2 2 12;2a				$MoPt_2$
S-AB_2X_3	2 2 12;2b				
β-$□Ga_2Se_3$	2 2 12;2c				
S-AB_3X_4	2 0 4;3				$CuPt_3$
S-AB_4X_5	0 2 8;4				$MoNi_4$
S-$ABCD_2X_5$	0 2 8;4	0 2 8;4	0 2 8;4	3 3 12;1.5	
$NiSi_2Cu_4S_7$	0 2 4;6	1 3 10;2.5	5.5 4.5 14;0.75		Mn_2Au_5

TABLE 1—*Continued*

Compound	$T_i(A)$	$T_i(B)$	$T_i(C)$	$T_i(D)$	Alloy
	B. Wurtzite-related structures				
ZnS	12 6 2;(1)				Mg
$Al_2(CO)$					
$(AgIn)S_2$					
$(CuCd_2Al)Se_4$					
W-AB_3X_4	0 6 2;3				$SnNi_3$
W-AB_3X_4	0 5 2;3				$CdAu_3$
$AsCu_3S_4$	0 4 2;3				$TiCu_3$
W-ABX_2	4 6 2;1				AuCd
W-ABX_2	4 5 2;1a				
W-ABX_2	4 5 2;1b				
β-$NaFeO_2$	4 4 2;1				
W-ABC_2X_4	0 6 2;3	0 6 2;3	4 6 2;1		
$GeCdCu_2S_4$	0 4 2;3	0 4 2;3	4 6 2;1		
$ZnSiNa_2O_4$	0 4 2;3	0 4 2;3	4 4 2;1		
$MgSiNa_2O_4$	0 4 2;3	0 4 2;3	4 4 2;1		
β-$CoSiLi_2O_4$	0 6 2;3	0 4 2;3	4 5 2;1a		
$ZnP□AgS_4$	0 6 2;3	0 4 2;3	0 6 2;3	0 4 2;3	
β-$(□ZnAl_2)S_4$	0 6 2;3	0 4 2;3	0 6 2;3	0 4 2;3	
W-ABX_2	9 3 0;1				
W-ABX_2	5 3 0;1				
α-LiSiNO	6 2 2;1				
W-ABX_2	6 0 2;1a				LiRh
W-ABX_2	6 0 2;1b				
α′-$□Ga_2S_3$	2 2 0;2a				
α-$□Al_2S_3$	2 2 0;2b				
$□GaInSe_3$	2 2 0;2b	2 2 0;2b	2 2 0;2b		
$SiLi_2O_3$	2 2 2;2				$TaPt_2$
$□B_2O_3$ II HP	2 2 2;2				$TaPt_2$
$□Si_2N_2O$	2 2 2;2				$TaPt_2$
W-AB_3X_4	2 0 2;3				$SbAg_3$
W-AB_4X_5	0 2 2;4				$ZrAu_4$
W-$ABCD_2X_5$	0 2 2;4	0 2 2;4	0 2 2;4	3 3 2;1.5	
$Si_2Cu_5S_7$	1 3 1;2.5				

Note. The T_i^N of the majority elements can be calculated from Eq. [1]. The metal atoms in parentheses, e.g., (Mn,In) in □(Mn, In)(Mn,In)$_2$Te$_4$ are disordered. Four sites with different ratios of □, Zn, and Al are occupied in β-$(□ZnAl_2)S_4$.

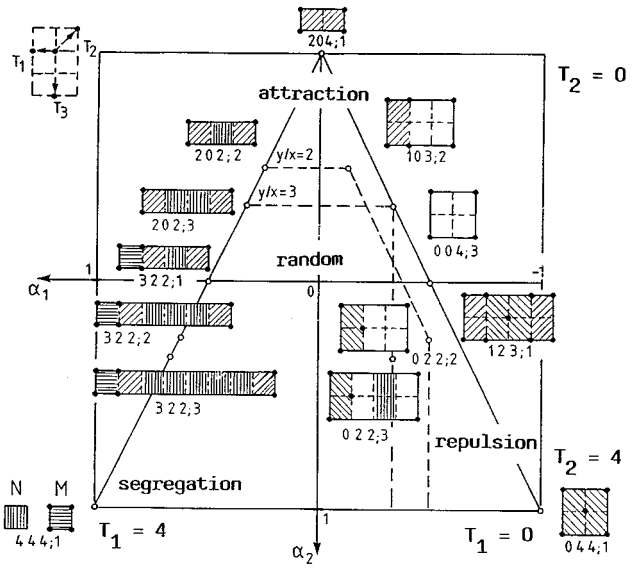

FIG. 2. α_1, α_2 structural map of ordered M_xN_y crystal structures $T_1T_2T_3;y/x$ of tetragonal layers with different shading of structural subunits containing 1–4 M atoms. T_1, T_2, and T_3 are the number of first, second and third neighbors shown on the upper left. The T_1,T_2 axes refer only to $y/x = 1$.

combined with squares containing two M atoms in *cis* configuration to the structures at the left side of the triangle. Points within the triangle are obtained by the combination of all the subunits.

(6) Structures $T_1T_2T_3;y/x$ with $y/x > 1$ values can be included in the same structure map (Fig. 2) by using the Cowley–Warren short-range order parameter α_i (4), which can vary within $-1 \leq \alpha_i \leq 1$. The α_i values can be obtained from the self-CN T_i^M and T_i^N of M and N atoms or from the T_i^M and y/x values (3):

$$T_i^N = T_i^{\max} - (T_i^{\max} - T_i^M)x/y, \qquad [1]$$

$$\alpha_i T_i^{\max} = T_i^M + T_i^N - T_i^{\max}, \qquad [2]$$

$$\alpha_i T_i^{\max} = T_i^M - (T_i^{\max} - T_i^M)x/y. \qquad [3]$$

The self-CN T_i^M and T_i^N of M and N atoms are identical at the composition $y/x = 1$ but different at other compositions. Structures with different compositions can be obtained by using a combination of structural subunits. The area mapped out by the maximum range of α_1, α_2 values is different at different compositions, as outlined for $y/x = 2$ and $y/x = 3$ in Fig. 2. The 0 0 4;3 structure at the corner of the structure map for $y/x = 3$ contains only squares with single occupancy. The 2 0 2;3 structure at the left corner contains squares with *cis* occupation or without M atoms similar to the case for $y/x = 1$. The structures at the right border as, for example, 0 2 2;3 can also be obtained by

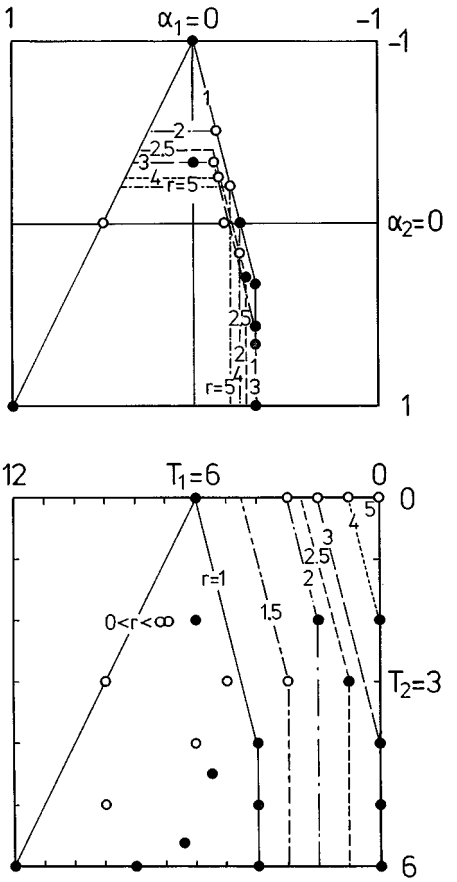

FIG. 3. Structural map of ordered $A_xB_yX_{x+y}$ adamantanes (●) and theoretical structures (○) with α_i values (above) and self-CN numbers T_i (below) of A atoms and composition $r = y/x$ as parameters. The boundary lines for different r values have the same dashing in both plots.

structural units similar to the case for $y/x = 1$, however with different concentrations of units containing zero, single, or double (*trans*) occupation.

The 2 0 2;2, 1 0 3;2, and 0 2 2;2 structures at the corners of the $y/x = 2$ field each consist of a combination of two structural units only. Structures at the borders as, for example, 3 2 2;2 or inside the $y/x = 2$ field contain three or more structural units, respectively.

(7) The α_i values are zero for a random distribution of M and N atoms, because the mean value of $T_i^M + T_i^N$ equals $T_i^{\max}$, which corresponds, for example, to $T_1 = T_2 = T_3 = 2$ at composition $y/x = 1$ (Fig. 2). Very small α_i values are expected for alloys with very weak interactions and in particular at high temperatures. Positive α_1 values are obtained for attractive interactions of M atoms, i.e., for cluster formation or segregation. The 2 0 2;2 and 3 2 2;2 structures of Fig. 2 consist of single and double rows of M atoms, respectively. The size of the M and N clusters is increased to complete segregation of M and N atoms in the 4 4 4;(1) structure. Negative α_1 values indicate repulsive interactions between M atoms, e.g., Coulomb repulsion.

3. ORDERED WURTZITE AND SPHALERITE STRUCTURES

Each Zn atom of the sphalerite structure with lattice constant a_0 has 12 nearest Zn neighbors at $a_0\sqrt{0.5}$, 6 next-nearest neighbors at a_0, and 24 third-nearest neighbors at distance $a_0\sqrt{1.5}$. In the undistorted hexagonal cell of wurtzite with $c = \sqrt{8/3}a$ each Zn atom has also 12 nearest and 6 next-nearest Zn neighbors at distances a and $a\sqrt{2}$, but only two third-nearest neighbors at c. The number T_1 of nearest neighbors corresponds to the number of ZnS_4 tetrahedra shared by corners. In $Cu_5Si_2S_7$, for example, with $T_1 = 1$, $T_2 = 3$, and $T_3 = 1$ Si atoms, each SiS_4 tetrahedron is linked to another SiS_4 tetrahedron in Si_2S_7 groups (Table 1). A maximum of $T_1 = 4$ neighbors occurs in experimental adamantane structures like β-$NaFeO_2$ and $CuFeS_2$ and $T_1 = 6$ in theoretical structures, In(Ga,Al) P_2 (7) and α-LiSiNO. Crystal structures with repulsive interactions of metal atoms exhibit a minimum of T_1 and a maximum of T_2 values, e.g., 4 6 2;1 and 0 6 2;3 in wurtzite or 4 6 8;1 and 0 6 0;3 in sphalerite structure (Fig. 3). The interactions between metal atoms can be characterized by the T_2 values, which vary from $T_2 = 6$ for repulsive to $T_2 = 0$ for attractive interactions. The structures listed in Table 1 are ordered for decreasing T_2. Equal T_1 and T_2 values, for example, of ccp $SbCu_3S_4$ (0 4 8;3) and hcp $AsCu_3S_4$ (0 4 2;3) or ccp $SnFeCu_2S_4$ (0 4 8;3, 0 4 8;3, 4 6 8;1) and hcp $GeCdCu_2S_4$ (0 4 2;3, 0 4 2;3, 4 6 2;1) indicate related structures with the possibility of complex stackings of metal atoms at substitution as, for example, $GeZnCu_2S_4$ (*ABACBCBACACB*) (2). The T_i values of Sb atoms in $SbCu_3S_4$ and Sn or Fe atoms in $SnFeCu_2S_4$ are identical. Also the concentration of Sb and Fe or Sn atoms relative to the remaining atoms is the same.

The structures of ccp $SbCu_3S_4$ and hcp $AsCu_3S_4$ are completely described by the self-CN 0 4 8;3 and 0 4 2;3 of the Sb and As atoms, respectively. The self-CN of the Cu atoms can be calculated by Eq. [1]. The ordering of the metal atoms $SbCu_3$ and $AsCu_3$ corresponds to the $TiAl_3$ and $TiCu_3$ structures (3). The ordering of Fe and Sn atoms, for example, in $SnFeCu_2S_4$ is the same as the ordering of Sb atoms in $SbCu_3S_4$ (0 4 8;3). There are, however, two possibilities for a combination of two atoms with the 0 4 8;3 structure as outlined for $SnZnCu_2S_4$ (Sn(Zn, Fe) Cu_2S_4) (kesterite) and $SnFeCu_2S_4$ (stannite) in Figs. 4a and 4b, respectively. In $SnZnCu_2S_4$ the Cu atoms have the same T_i values (4 4 16;1) as the Cu atoms in $CuFeS_2$ (Fig. 4a), whereas the T_i values (4 6 8;1) of Cu atoms in $SnFeCu_2S_4$ correspond to those of In atoms in $\square Cd\,In_2Se_4$ (Fig. 4b). The $SnFeCu_2S_4$, β-$\square HgCu_2I_4$, and $\square(Mn, In)(Mn, In)_2Te_4$ structures exhibit the same ordering of metal atoms and vacancies $\square$. The formulas are written somewhat differently as usual (Cu_2FeSnS_4, β-Cu_2HgI_4, and $(MnIn_2)Te_4$) (1, 2) to indicate the structural relation between the different compounds and the relation to alloy structures (Table 1). The sequence of metal atoms corresponds to increasing concentration of metal atoms as, for example, $NiSi_2Cu_4S_7$ or $\square Cd\,In_2Se_4$ in the present investigation (instead of increasing valence as, for example, $Cu_4NiSi_2S_7$ and $Cd\,In_2Se_4$ (1, 2)). The ordering of vacancies and metal atoms of $\square Cd\,In_2$ in $\square Cd\,In_2Se_4$, for example, corresponds to the $PdAuCu_2$ alloy structure (3). The T_i values of $\square$ and Cd in $\square Cd\,In_2Se_4$ are 0 6 0;3 (Fig. 4).

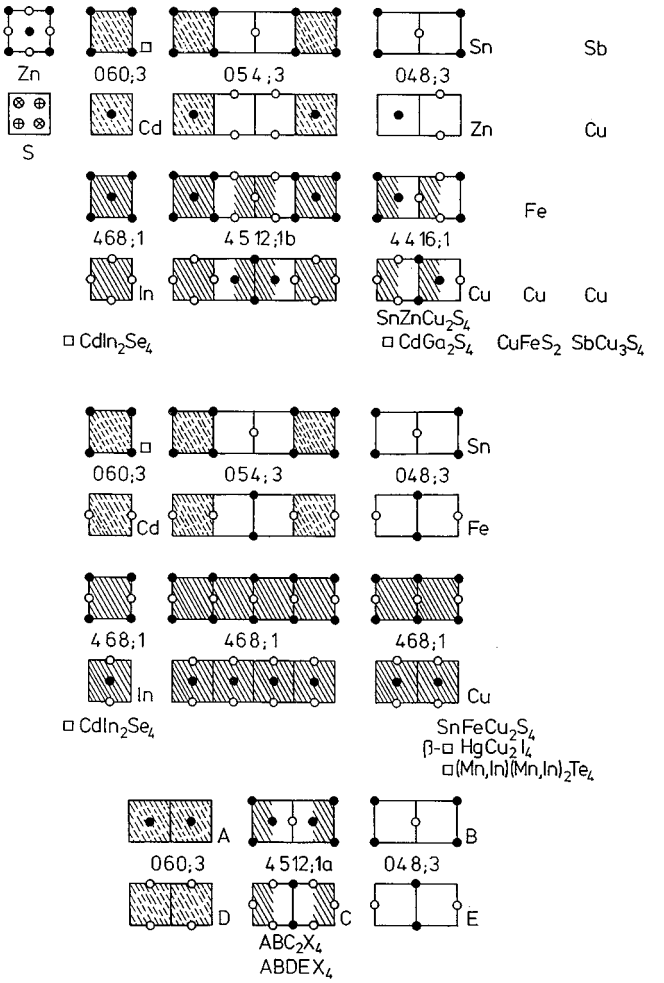

FIG. 4. Projection of the face-centered cubic sphalerite structure with Zn atoms at projection height $z = 0$ (●) and $z = 0.5$ (○) and S atoms at $z = 0.25$ (⊗) and $z = 0.75$ (⊕). Positions of metal atoms and three different combinations a (upper part), b (middle part), and c (lower part) of structural units (dashed and white areas) at the right border of the structural map (Fig. 3).

4. COMBINATION OF STRUCTURAL UNITS

The 0 6 0;3 and 0 4 8;3 structures correspond to the $AuCu_3$ and $TiAl_3$ structures (3). The structural units can be combined to form the 0 5 4;3 $ZrAl_3$ structure as shown in Figs. 4a and 4b. The 4 6 8;1 CuAu and the 4 4 16;1 U Pb (or

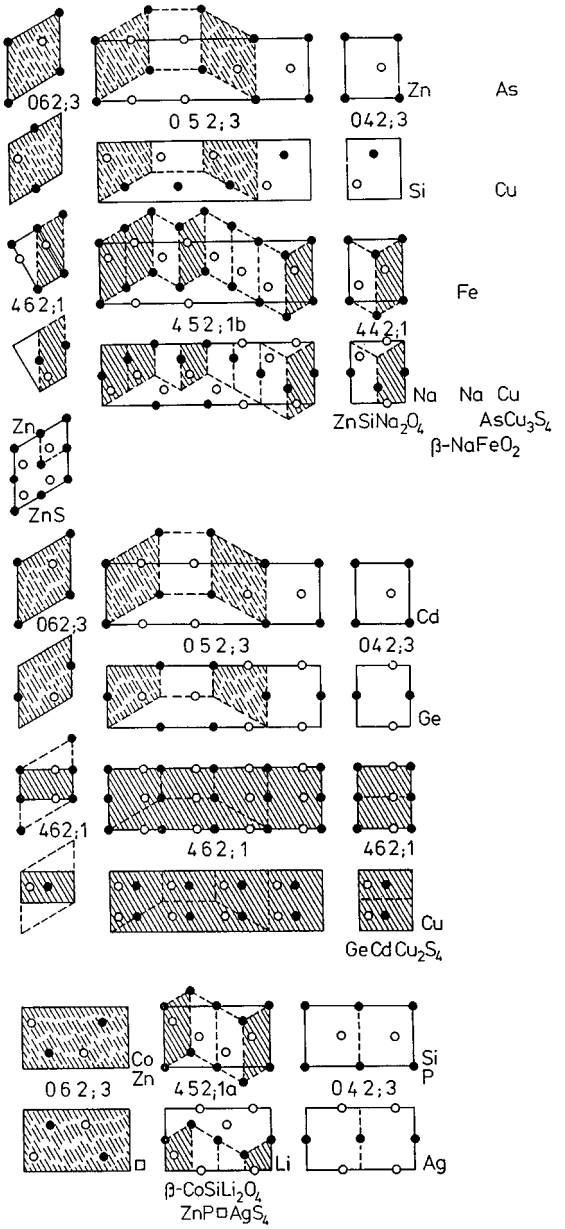

FIG. 5. Projection of metal atoms at A (●) and B (○) positions of ordered $A_xB_yX_{x+y}$ wurtzite structures (Fig. 1) and the three different combinations a (upper part), b (middle part), and c (lower part) of structural units at the right border of the structural map (Fig. 3).

$CuFeS_2$) structural units can be combined in a similar way to form, for example, the 4 5 12;1b structure. The four structural units 0 6 0;3, 0 4 8;3, 4 6 8;1 and 4 4 16;1 are combined in some alloys such as $ZrGa_2$, $HfGa_2$, $ZrSi_2$, and Nb_5Ga_{13} to obtain compositions between AB and AB_3 ($1 \leq y/x \leq 3$) (3). In adamantane structures two 0 6 0;3 structures are combined to form the 4 6 8;1 structure in $\square CdIn_2Se_4$, or two 0 4 8;3 structures are combined to form the 4 4 16;1 structure in $SnZnCu_2S_4$ (Fig. 4a). A different combination always yields the 4 6 8;1 structure as outlined in Fig. 4b. The 0 6 0;3 and 0 4 8;3 structural units, however, can also be combined to form the 4 5 12;1a structure as outlined in Fig. 4c. The corresponding series of wurtzite-related structures (Figs. 5a–c) will be discussed later.

5. HOMOMETRIC STRUCTURES

The α'-$\square Ga_2S_3$ (2 2 0;2a) structure and the α-$\square Al_2S_3$ (2 2 0;2b) structure (Fig. 6) have identical T_i values of all atoms for all i. The homometric structures cannot be distinguished by powder diffraction methods if the lattice is undistorted (3). Other structures are enantiomorphous; i.e. the crystal structures contain right- or left-hand screw axes that cannot be distinguished by powder diffraction. The homometric, but nonenantiomorphous, structures are characterized by adding a suffix a, b, or c to their coordination description. The ccp structures corresponding to 2 2 0;2a and 2 2 0;2b are $GeCu_2Se_3$ and AB_2X_3 with 2 2 12;2a and 2 2 12;2b (Figs. 6 and 7a). The β-$\square Ga_2Se_3$ structure 2 2 12;2c is different from the homometric 2 2 12;2a,b structures in the sixth and higher coordination shells. We call this property *quasi-homometric*.

The lattice energy of these structures should differ only by small amounts. Other examples of homometric structures are ccp 6 0 12;1a,b and 6 2 12;1a,b (3), whereas, for example, 4 5 12;1a,b (Fig. 4) or the hcp structures 4 5 2;1a,b (Fig. 5) and 6 0 2;1a,b (3) are quasi-homometric and differ in higher coordination shells.

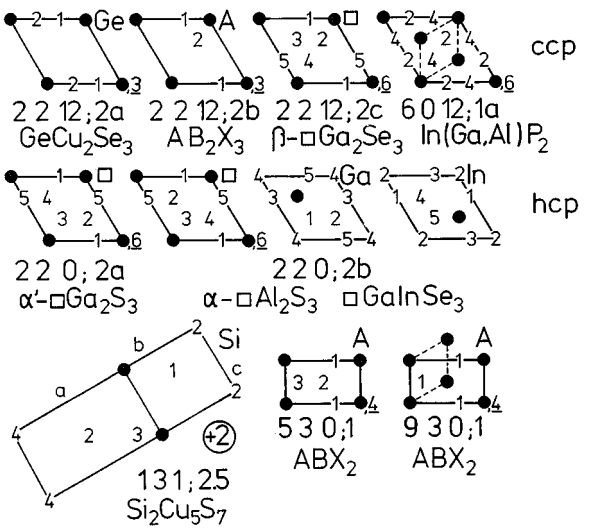

FIG. 6. Projection of metal atoms in ordered ccp sphalerite (upper part) and hcp wurtzite structures (lower part) for layer number 0 (●),1,2, … with the underlined value for the corresponding $c_{hex} = 3$ or 6 layers, respectively as outlined in Fig. 1. The a and b axes of the $Si_2Cu_5S_7$ structure are pointing to atoms in the fourth or second layer, respectively. The number 2 should be added to all numbers to indicate the second Si atom of the Si_2S_7 groups.

6. HOMOLOGOUS SERIES OF STRUCTURES

A second type of special structure exhibits identical α_i values, but at different composition y/x. These structures have identical or closely related unit cells and form homologous series of structures that are filled up successively by M atoms until $T_i^{\max}$ is reached. Each M and each N atom of these structures must have the same set of numbers T_1, T_2, T_3, respectively. The structure with the lowest M content $y/x = r$, $T_1^* T_2^* T_3^*;r$, is filled up with M atoms in steps of $k = r, r-1, \ldots, 0$

$$T_i(k) = T_i^{\max} - (T_i^{\max} - T_i^*)k/r, \qquad [4]$$

$$y/x = k(r + 1 - k). \qquad [5]$$

Two examples of homologous series of ccp structures are $T_1^* T_2^* T_3^*;r =$ 0 6 0;3 (Fig. 4a) and 0 2 8;4 (Fig. 7a). The sequences of structures 0 6 0;3, 4 6 8;1, 8 6 16;0.33, 12 6 24;(1) and 0 2 8;4, 3 3 12;1.5, 6 4 16;0.67, 9 5 20;0.25, 12 6 24;(1) contain also T_i values of majority components with $y/x < 1$, as, for example, 8 6 16;0.33 of Cu atoms in the $AuCu_3$ structure.

Some other series of structures are very similar to the homologous series, but differ in the fourth or higher self-CN T_i. We call them *quasi-homologous*. An example is the hcp series 0 2 2;4, 3 3 2;1.5, 6 4 2;0.67, 9 5 2;0.25, 12 6 2;(1), which is closely related to the homologous ccp series (Figs. 7a,b).

7. NON-HOMOLOGOUS SERIES OF STRUCTURES

Ternary adamantane structures $A_xB_yX_{x+y}$ are always homologous, as we have demonstrated before. The α_i values of the A and B atoms are identical. In quaternary compounds (or ternary compounds containing vacancies) such as $ZnSiNa_2O_4$ (Fig. 5a), the T_i values of Zn or Si atoms (0 4 2;3) and Na atoms (4 4 2;1) correspond to different α_i values (Fig. 3). A different combination of atoms with the 0 4 2;3 structure yields the T_i values 4 6 2;1 in $GeCdCu_2S_4$ (Fig. 5b). Also different structures, e.g., 0 4 2;3 and 0 6 2;3, can be combined in few cases as is shown for the β-$CoSiLi_2O_4$ structure in Fig. 5c. Only half of the Li positions are occupied in the $ZnP\square AgS_4$ structure. β-$\square ZnAl_2S_4$ seems to be isotypic, with a mixed occupation of Zn and Al atoms at the four sublattices. The corresponding ccp structures were mentioned in Section 3.

8. ISING-TYPE ANALYSIS

The self-CN T_i of the adamantane structures are plotted in structure maps in Fig. 3. Corresponding wurtzite- and sphalerite- related structures have identical T_1 and T_2 values and differ only in T_3 and higher T_i values. The three-dimensional hexahedron of hcp structures with $y/x = 1$ contains at the corners the 5 3 0;1 and 9 3 0;1 structures in addition to the 12 6 2;(1), 6 0 2;1, 4 4 2;1, and 4 6 2;1 structures of the T_1, T_2 map. With 6 corners, 6 planes, and 10 edges, it obeys Euler's rule $C + P = E + 2$. The 6 2 2;1 structure of α-LiSiNO lies on the surface of the

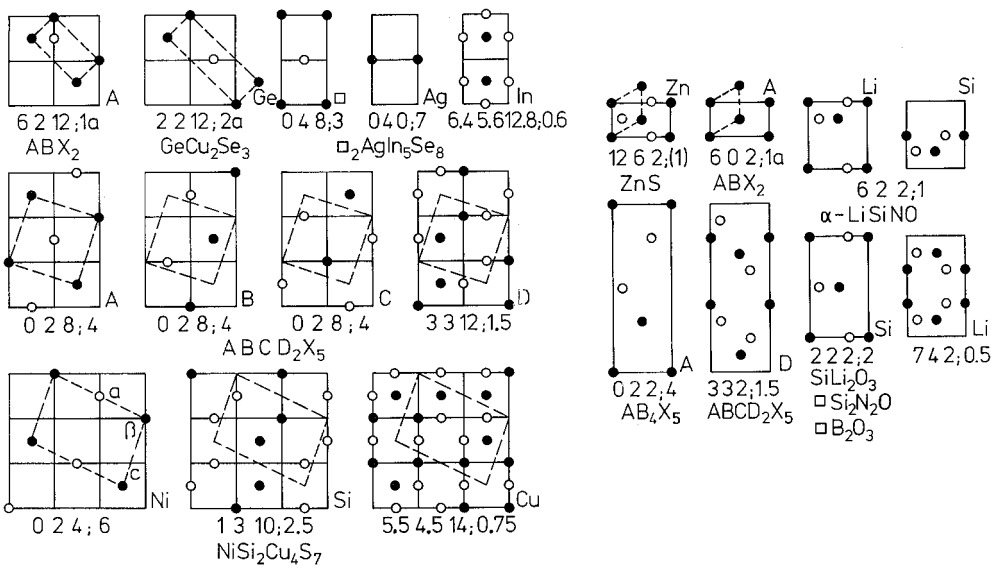

FIG. 7. Projection of sphalerite (a, left part) and wurtzite (b, right part) derivative structures similar to Figs. 4 and 5, respectively.

hexahedron. Structures with low T_2 values such as 6 0 2;1 or 6 2 2;1 (α-LiSiNO) indicate attractive interactions between Li atoms, whereas structures with high T_2 values such as 4 6 2;1 or 4 4 2;1 (β-$NaFeO_2$) indicate repulsive interactions between Na atoms.

9. VALENCE AND ELECTROVALENCE OF METAL ATOMS IN ADAMANTANE STRUCTURES

The Zn and S atoms of ZnS (2 6) contain $e_A = 2$ and $e_X = 6$ (A = Zn, X = S) electrons, which can form four bonds with a total of eight electrons. The eight electrons are also contributed in GaAs (3 5), Cu I (1 7), or diamond (4 4). In a ternary or quaternary adamantane structure $A_uB_vC_wD_yX_n$ ($u + v + w + y = n$) the sum of the electrons should be 8 or a multiple of 8 (1, 2):

$$ue_A + ve_B + we_C + ye_D + ne_X = 8n, \qquad [6]$$

as, for example, in $CuFeS_2$ (1 3 6_2), Cu_2GeSe_3 (1_2 4 6_3), or Cu_3AsS_4 (1_3 5 6_4). The substitution of trivalent Ga in GaAs (3 5) yields $CdGeAs_2$ (2 4 5_2) or $CuGe_2P_3$ (1 4_2 5_3) (1, 2, 8).

In defect adamantane structures with $A = \square$, the number of vacancies $\square$ should not exceed $u/n = 3/8$ because of the destabilization of the nonbonding orbitals (1, 2). Compounds such as $\square Cd\,In_2Se_4$ (0 2 3_2 6_4), β-$\square Ga_2Se_3$ (0 3_2 6_3), or $\square_3Ga_4GeSe_8$ (0_3 3_4 4 6_8) with $u/n = 0.25$, 0.33, or 0.375 were observed (1, 2). The equation for electroneutrality

$$ue_A + ve_B + we_C + ye_D = n(8 - e_X) \qquad [7]$$

is identical to Eq. [6] and allows also formulas such as 0 3_2 6_3, 0 4_3 5_4, or 0 1_2 2 7_4 (β-$\square Cu_2Hg\,I_4$).

Pauling's electrovalence rule requires that the electrovalence $s = e_i/CN$ of the metal atoms with charge e_i and coordination number CN = 4 is compensated locally by the charge of each anion $8 - e_X$ (1, 2, 5). Therefore the sum of the charges of the four metal atoms (or vacancies in defect adamantane structures) should be 4, 8, or 12 for each mono-, di-, or trivalent anion in a structure.

The analysis of the different adamantane structures shows that Pauling's rule is satisfied for all structures shown in Figs. 4 and 5 and deviates by $\Delta \geq 0.25$ in other structures. The structures shown in Figs. 4 and 5 are all at the right border of the structure map with $3\alpha_1 + 1 = 0$ (Fig. 3). In NaCl-related structures Pauling's rule was satisfied for the upper right border of the map with $4\alpha_1 + \alpha_2 + 1 = 0$ (3, 6).

The tendency to small numbers M^i of metal atoms with different environments $T_1T_2T_3$ satisfies Pauling's rule of parsimony: the number of essentially different kinds of constituents in a crystal tends to be small (5). The structures with one or two different environments of metal atoms also have the highest symmetry. The structures of $CuFeS_2$ (4 4 16;1) and $\square Cd\,In_2Se_4$ (4 6 8;1 of In atoms), for example, have a higher symmetry than the combination of both, like 4 5 12;1a or 4 5 12; 1b (Figs. 4a and 4c). The structures shown in Figs. 4 and 5 are examples where Pauling's rules are obeyed at combinations of metal atoms to ternary or quaternary compounds. In other structures such as $\square_2AgIn_5Se_8$ or $NiSi_2Cu_4S_7$, the In or Cu atoms, respectively, have different environments $T_1T_2T_3$ and do not obey Pauling's rules. The rules are also not obeyed for In (3.7 3.7 11.1;1.5) or Cu,In atoms (6.4 3.2 9.6;1.1) in $\square Cu_3In_{13}$ $(Cu, In)_{15}Se_{32}$ or the metal atoms of $\square_{15}Cd_{13}In_{26}Se_{54}$ (1, 2).

10. CONCLUSIONS

The ordering of metal atoms in sphalerite- and wurtzite-related structures is compared with the ordering of metal atoms in cubic- and hexagonal-close-packed structures (Table 1). The location of the metal atoms in undistorted structures can be characterized by the self-coordination numbers T_1, T_2, and T_3, which are plotted on structure maps (Fig. 3). Most compounds with composition ABX_2, AB_3X_4, ABC_2X_4, or $ABCDX_4$ are at the right border of the map and satisfy Pauling's electrovalence rule. The minimum T_1 values indicate repulsive interactions between the metal atoms. A few compounds such as $In(Ga,Al)P_2$ with an ordering of In and (Ga,Al) atoms similar to CuPt (7) or α-LiSiNO with self-CN 6 0 12;1a or 6 2 2;1 (Table 1) exhibit attractive interactions between metal atoms because of the increased $T_1 = 6$ and decreased T_2 values. Compounds with composition AB_2X_3 such as $GeCu_2Se_3$ or β-$\square Ga_2Se_3$ with self-CN 2 2 12;2 (ccp), 2 2 0;2, or 2 2 2;2 (hcp) are at intermediate positions. The self-CN values of other compounds such as $\square Cu_3In_{13}(Cu, In)_{15}Se_{32}$ or $\square_{15}Cd_{13}In_{26}Se_{54}$ (1, 2) are inside the T_1,T_2,T_3 polyhedron and indicate incomplete ordering. These structures do not obey Pauling's rule of parsimony as was outlined in Section 9.

Also Pauling's rule of parsimony seems to be important for the composition. Most compounds contain metal atoms with a single or two different valencies. Four to seven different compositions for pnictides, chalcogenides, and halogenides and a choice of metal atoms with proper valency are shown in Fig. 8. The quaternary compounds are at the lines which are connecting two corners of ternary compounds. The quinary compounds are within triangles as is outlined, for example, by dashed lines for $ZnP\square AgS_4$ (0 1 2 5 6_4). Three formula units 0_3 1_3 2_3 5_3 6_{12} can segregate to the binary and ternary compounds ZnS (2 6), $\square_3P_2S_5$ (0_3 5_2 6_5), and Ag_3PS_4 (1_3 5 6_4) if these compounds exhibit an increased stability. Ternary adamantanes with more than 37.5 % vacancies such as 0_3 5_2 6_5 are shown in parentheses because of the instability (1, 2). The ternary compounds have the composition ABX_2, AB_2X_3, AB_3X_4 or $A_2B_3X_5$ (0_3 5_2 6_5). Most quaternary compounds contain four

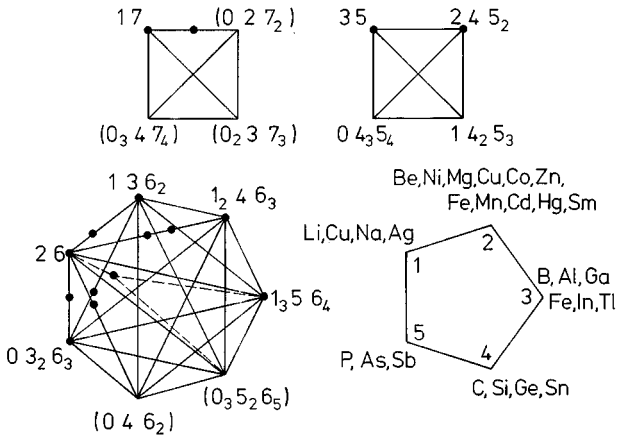

FIG. 8. Valency of atoms in adamantane structures in the order of increasing tetrahedral radii (9) (right) and composition of binary, ternary, quaternary, and quinary compounds as, for example, 2 6, 1 3 6_2, 1 2_2 3 6_4, and 0 1 2 5 6_4 (left). The point between 2 6 and 0 3_2 6_3 composition, for example, corresponds to 0 2 3_2 6_4 composition of, for example, $\square CdGa_2S_4$. The quinary composition 0_3 1_3 2_3 5_3 6_{12} of three formula units of $\square AgZnPS_4$ (= $ZnP\square AsS_4$) can be obtained by combination of ZnS (2 6), $\square_3P_2S_5$ (0_3 5_2 6_5), and Ag_3PS_4 (1_3 5 6_4) as outlined by the dashed lines. The compositions of unstable compounds with more than 37.5% vacancies [1, 2] such as 0_3 5_2 6_5 are in parentheses.

X atoms, e.g., $\square CdIn_2Se_4$ (0 2 3_2 6_4), $SnFeCu_2S_4$ (1_2 2 4 6_4), or β-$\square HgCu_2I_4$ (0 1_2 2 7_4). A few quaternary compounds, for example, $\square CuIn_3Te_5$ (0 1 3_3 6_5) (8), $NiSi_2Cu_4S_7$ (1_4 2 4_2 6_7), and $\square_2AgIn_5Se_8$ (0_2 1 3_5 6_8), have more than four *X* atoms. The compounds containing five *X* atoms as, for example, $\square CuIn_3Te_5$ (0 1 3_3 6_5) (8) or the theoretical compound Cu_3ZnSbS_5 (1_3 2 5 6_5) could crystallize in the homologous S-A_3BCX_5 structure as was outlined in Section 6. In the present nomenclature 1_4 2 4_2 6_7 $Si_2Cu_5S_7$ is a quaternary compound similar to $NiSi_2Cu_4S_7$ (Table 1) with four monovalent and one divalent Cu atom. Also Fe can occur in different valencies as in $\square FeGa_2Se_4$ (0 2 3_2 6_4) or β-$NaFeO_2$ (1 3 6_2) (1, 2, 8). The selection of the proper elements listed in Fig. 8 and the choice of the appropriate $p(X_2)$ partial pressure might help to synthesize new compounds and to investigate compounds containing elements with unusual valency. New techniques such as the deposition of thin epitaxial films by MOCVD allow the synthesis at lower temperatures than the usual technique of annealing mixtures. In(Ga,Al)P_2, for example, can be obtained at $\approx 730^\circ$C (7). This compound with nomenclature (3 3′ 5_2) contains larger In atoms in hexagonal layers, whereas Ga and In atoms of $\square GaInSe_3$ (0 3 3′ 6_3) are ordered in each layer (Fig. 6).

The comparison of the compounds in Table 1 with corresponding self-CN values, for example, $SbCu_3S_4$ (0 4 8;3) and $AsCu_3S_4$ (0 4 2;3) or $CuFeS_2$ (4 4 16;1) and β-$NaFeO_2$ (4 4 2;1), shows that the compounds containing the smaller atoms As instead of Sb or O instead of S usually favor a wurtzite-related structure. A variation of the size, for example, in $AsCu_3S_4$–$SbCu_3S_4$ solid solution could favor a complex stacking variation as was outlined in Section 1, other ordered structures as, for example, 1_6 3 3′ 6_8, or a segregation corresponding to Pauling's rule of parsimony. An increasing number of metal atoms with different size and valency reduces the possibility of finding a proper adamantane structure with close packing of metal atoms.

REFERENCES

1. E. Parthé, *in* "Intermetallic Compounds" (J. H. Westbrook and R. L. Fleischer, Eds.) Vol. 1, p. 343. Wiley, London, 1994.
2. E. Parthé, L. Gelato, B. Chabot, M. Penzo, K. Cenzual, R. Gladyshevskii, "Gmelin Handbook of Inorganic and Organometallic Chemistry," Vol. 1. Springer, Berlin, 1993.
3. J. Hauck and K. Mika, *in* "Intermetallic Compounds" (J. H. Westbrook and R. L. Fleischer, Eds.), Vol. 1, p. 277. Wiley, London, 1994.
4. F. Ducastelle, "Cohesion and Structure" (F. R. de Boer and D. G. Pettifor, Eds.), Vol. 3. North-Holland, Amsterdam, 1991.
5. L. Pauling, *J. Am. Chem. Soc.* **51,** 1010 (1929).
6. J. Hauck, D. Henkel, and K. Mika, *Z. Kristallogr.* **182,** 297 (1988).
7. T. Hauck, unpublished.
8. P. Villars and L.D. Calvert, "Pearson's Handbook of Crystallographic Data for Intermetallic Phases," Vols. 1–3. American Society for Metals, Metals Park, OH, 1986.
9. R.D. Shannon, *Acta Crystallogr., Sect. A* **32,** 751 (1976).